

Optimal Blind Nonlinear Least-Squares Carrier Phase and Frequency Offset Estimation for General QAM Modulations

Yan Wang, Erchin Serpedin, *Member, IEEE*, and Philippe Ciblat

Abstract—This paper introduces a family of blind feedforward nonlinear least-squares (NLS) estimators for joint estimation of the carrier phase and frequency offset of general quadrature amplitude modulated (QAM) transmissions. As an extension of the Viterbi and Viterbi (V&V) estimator, a constellation-dependent optimal matched nonlinear estimator is derived such that its asymptotic (large sample) variance is minimized. A class of conventional monomial estimators is also proposed. The asymptotic performance of these estimators is established in closed-form expression and compared with the Cramér–Rao lower bound. A practical implementation of the optimal matched estimator, which is a computationally efficient approximation of the latter and exhibits negligible performance loss, is also derived. Finally, computer simulations are presented to corroborate the theoretical performance analysis and indicate that the proposed optimal matched nonlinear estimator improves significantly the performance of the classic fourth-power estimator.

Index Terms—Blind estimation, carrier phase, frequency offset, quadrature amplitude modulated (QAM) constellations, synchronization.

I. INTRODUCTION

QUADRATURE amplitude modulation (QAM) is a highly bandwidth efficient transmission technique for digital communications. Currently, large QAMs are widely used in throughput efficient high-speed communication applications such as digital television and time-division multiple access systems. One of the problems associated with the use of large QAM modulations is that of carrier recovery, which for efficiency reasons must be performed without using preambles [8], [18], [20], i.e., in a blind or nondata-aided (NDA) mode.

Carrier recovery involves the acquisition of both the carrier frequency and phase. Recently, assuming that the frequency recovery has already been achieved, a number of blind feedforward phase estimators for square and cross-QAM modulations were reported in [3]–[8], [12, pp. 281–282], and [15], and analyzed in [18] and [20]. These estimators exploit the angle information contained in the fourth-order or higher order statistics of the

received signal. Reference [20] has shown that the seemingly different estimators [3], [12, pp. 281–282], and [15] are equivalent to the standard fourth-power estimator, while the estimator [5] exhibits a larger asymptotic (large sample) variance than the former class [3], [15]. A so-called reduced-constellation (RC) fourth-power algorithm, which slightly improves the performance of the classic fourth-power estimator, is proposed in [8]. However, it is well-known that both the RC and the standard fourth-power estimators exhibit relatively poor performance in the case of cross-QAM transmissions [8]. Also, [8] introduces two signal-to-noise ratio (SNR)-dependent methods that outperform the performance of standard and RC fourth-power estimators in the case of cross- and square-QAM constellations, at moderate to high SNR levels, respectively. However, in the case of square-QAM constellations and low SNRs, the performance of these two methods is inferior to the fourth-power algorithm [8].

This paper proposes a family of NDA feedforward nonlinear least-squares (NLS) estimators for joint phase and frequency offset estimation of carriers that are fully QAM-modulated. The proposed NLS estimators represent a generalized form of a low SNR-approximation of the maximum likelihood (ML) estimator, that was originally proposed by Viterbi and Viterbi (V&V) as a blind carrier phase estimator for fully modulated phase-shift keying (M-PSK) transmissions [16], [22]. This carrier phase estimator is referred in the literature as the V&V algorithm [12, p. 280]. Based on the V&V algorithm, Efstathiou and Aghvami have introduced blind carrier phase and frequency offset estimators for 16-QAM modulated transmissions [6], [7], which are similar to the RC fourth-power algorithm in the sense that they tend to emphasize the weight of the four corner points in the signal constellation. Morelli *et al.* pointed out that this solution was unsatisfactory with short bursts and proposed a new blind scheme with superior performance to previous methods [13]. However, it appears that it is not straightforward to extend this algorithm to general QAM modulations that are different from 16-QAM.

In this paper, we introduce optimal “matched” estimators as well as computationally efficient approximate matched carrier estimators for general square and cross-QAM modulations. The proposed matched estimators are constellation-dependent and are optimally designed such that their asymptotic variance is minimized. The performance of these matched algorithms is compared with the Cramér–Rao bound (CRB), calculated according to [18], and shown that the optimal matched estimator exhibits superior performance [smaller symbol error rate (SER)]

Manuscript received December 21, 2001; revised June 14, 2002; accepted October 6, 2002. The editor coordinating the review of this paper and approving it for publication is D. Goeckel. This work was supported by the National Science Foundation under Award CCR-0092901.

Y. Wang and E. Serpedin are with the Department of Electrical Engineering, Texas A&M University, College Station, TX 77843-3128 USA (e-mail: serpedin@ee.tamu.edu).

P. Ciblat is with the Department Communications and Electronics, Ecole Nationale Supérieure des Télécommunications, Paris F-75013, France.

Digital Object Identifier 10.1109/TWC.2003.816775

with respect to the classic fourth-power estimator at any SNR level, but significant improvements are observable especially at medium and high SNRs. The proposed estimation techniques represent a quite general and unifying framework to design blind carrier synchronizers with improved performance. It appears that some of the existing synchronizers [13], [19] may be obtained as special cases of the proposed estimation framework.

The rest of this paper is organized as follows. In Section II, the discrete-time channel model is described. Section III introduces the family of blind NLS joint carrier phase and frequency offset estimators for general square-QAM constellations. The asymptotic performance of these estimators is established in closed-form expression and exploited to develop optimal matched nonlinear estimators that exhibit minimum variance. A class of conventional monomial estimators is proposed and their asymptotic performance established in closed-form expression, too. This family of estimators is further extended to general cross-QAM constellations in Section IV. Section V presents a unifying approach for designing computationally efficient approximations of the proposed optimal matched estimator. In Section VI, simulation results are conducted to confirm our theoretical analysis and show the superior performance of the proposed optimal estimator. Finally, in Section VII, conclusions are drawn and detailed mathematical derivations of the proposed performance analysis are reported in the appendixes.

II. PROBLEM FORMULATION

We consider a baseband QAM communication system where the filtering is evenly split between transmitter and receiver so that the overall channel satisfies the first Nyquist condition. Sampling the receiver output at the right time instants yields¹

$$\begin{aligned} x(n) &= w(n)e^{j\eta(n)} + v(n), \quad n = 0, \dots, N-1 \\ \eta(n) &:= \theta + 2\pi F_e T n \end{aligned} \quad (1)$$

where $\{w(n)\}$ is the independently and identically distributed (i.i.d.) input M-QAM symbol stream with zero-mean and unit variance ($\sigma_w^2 := E\{|w(n)|^2\} = 1$), T denotes the symbol period, $\{v(n)\}$ is a zero-mean circular white Gaussian noise process independent of $w(n)$ and with variance $\sigma_v^2 := E\{|v(n)|^2\}$, and θ and $f_e := F_e T$ stand for the unknown carrier phase and frequency offset, respectively, which are the parameters to be estimated based only on knowledge of received samples $\{x(n)\}_{n=0}^{N-1}$. The SNR per symbol is defined as $\text{SNR} := 10 \log_{10}(\sigma_w^2/\sigma_v^2)$.

Because the input QAM constellation has quadrant ($\pi/2$) symmetry, it follows that the estimates of θ and F_e present four-fold ambiguities, which can be counteracted by applying differential encoding. Without any loss of generality, we assume that the unknown phase θ lies in the interval $(-\pi/4, \pi/4)$ and $|f_e| < 1/8$. The estimation approach that we will pursue consists of exploiting a nonlinear transformation on the received signal samples $x(n)$ to remove the unwanted multiplicative modulation-introduced effects due to the transmit random

symbols. It turns out that the resulting problem reduces to the standard problem of estimating the phase parameters of a constant amplitude harmonic embedded in additive noise, for which standard NLS-type estimators can be developed and their asymptotic variance can be established in closed-form expression. The key element in deriving the optimal estimator is to select the optimal nonlinear transformation so that the estimator's asymptotic variance is minimized.

III. ESTIMATORS FOR SQUARE QAM CONSTELLATIONS

A. Matched Nonlinear Carrier Synchronizer

First, let us consider square-QAM constellations (i.e., with sizes $M = 2^{2m}$, $m = 1, 2, \dots$). With normalized energy, $w(n)$ takes a value from the set $(1/r_w)\{\pm(1+2l) \pm j(1+2k)\}$, $(l, k) \in \mathcal{A}_M\}$ with $\mathcal{A}_M := \{(0, 1, 2, \dots, 2^{m-1} - 1)^2\}$ and

$$r_w^2 := \frac{4}{M} \sum_{(l,k) \in \mathcal{A}_M} [(1+2l)^2 + (1+2k)^2].$$

Represent $x(n)$ in its polar form

$$x(n) = \rho(n)e^{j\phi(n)} \quad (2)$$

and define the process $y(n)$ via the nonlinear transformation

$$y(n) := F(\rho(n))e^{j4\phi(n)} \quad (3)$$

where $F(\cdot)$ is a real-valued nonnegative arbitrary nonlinear function. We will show shortly that $y(n)$ can be interpreted as a constant amplitude harmonic embedded in additive noise, and the unknown carrier phase can be extracted from the parameters (phase/frequency) of this constant amplitude harmonic. It is interesting to remark that the transformation (3) differs from the class of nonlinear transformations introduced in [16] and [22]. This difference is due to the fact that all QAM constellations exhibit quadrant symmetries which translate into nonzero fourth-order moments ($E\{w^4(n)\} \neq 0$), and consequently justify the special form of the exponential factor in (3).

Conditioned on the transmitted signal $w(n)$, $x(n)$ is normally distributed with the probability density function (pdf) $f(x(n)|w(n)) \sim \mathcal{N}(w(n)\exp(j\eta(n)), \sigma_v^2)$. Throughout the paper, the notation $f(\cdot)$ will stand for the pdf of certain random variables (RVs). Due to (2), it follows that

$$\begin{aligned} f(\rho(n), \phi(n)|w(n)) &= \rho_w(n)e^{j\phi_w(n)} \\ &= \frac{\rho(n)}{\pi\sigma_v^2} e^{-(\rho^2(n) + \rho_w^2(n))/\sigma_v^2} e^{(2\rho(n)\rho_w(n)\cos[\phi(n) - \phi_w(n) - \eta(n)])/\sigma_v^2} \end{aligned} \quad (4)$$

where $\rho_w(n)$ and $\phi_w(n)$ denote the amplitude and phase angle of $w(n)$, respectively. Based on (4), it is easy to infer that the joint and marginal pdf of $\rho(n)$ and $\phi(n)$ take the expressions shown in (5) and (6), at the bottom of the next page, where $\varrho_{l,k} := \sqrt{[(1+2l)^2 + (1+2k)^2]}/r_w$, $\psi_{l,k} := \arctan((1+2k)/(1+2l))$, and $I_0(\cdot)$ stands for the zeroth-order modified Bessel function of the first kind [1, eq. (9.6.16)]. Moreover, since $w(n)$ and $v(n)$ are i.i.d. and mutually independent, based on (1) and (2), it is not difficult to find that the joint pdf of

¹Notation $:=$ stands for "is defined as."

the RVs $\rho(n_1)$, $\phi(n_1)$, $\rho(n_2)$, $\phi(n_2)$ satisfies the following factorization:

$$f(\rho(n_1), \phi(n_1), \rho(n_2), \phi(n_2)) = f(\rho(n_1), \phi(n_1)) \cdot f(\rho(n_2), \phi(n_2)), \quad \text{for } n_1 \neq n_2. \quad (7)$$

Exploiting (5), some calculations, whose details are provided in Appendix I, lead to the following relations:

$$E\{y(n)\} = E\{F(\rho(n))e^{j4\phi(n)}\} = C e^{j(\pi+4\eta(n))} \quad (8)$$

$$C := |E\{y(n)\}| = |E\{F(\rho(n))e^{j4\phi(n)}\}| \quad (9)$$

where the amplitude C is a real-valued constant which does not depend on n . Since $w(n)$ and $v(n)$ are i.i.d. and mutually independent, from (7), it follows that $u(n) := y(n) - E\{y(n)\}$ is wide sense stationary (WSS) i.i.d., too. Consequently

$$y(n) = C e^{j(\pi+4\eta(n))} + u(n), \quad n = 0, 1, \dots, N-1 \quad (10)$$

and $y(n)$ can be viewed as a constant amplitude harmonic embedded in additive WSS white noise. Note that, in general, the WSS white noise process $u(n)$ is neither Gaussian distributed nor circular [17].

Let $\boldsymbol{\omega} := [\mu \ \omega_0 \ \omega_1]^T = [-C \ 4\theta \ 8\pi f_e]^T$ and $\bar{\boldsymbol{\omega}}$ be the trial value of $\boldsymbol{\omega}$, and introduce the following NLS estimator (see, e.g., [2], [9], and [21]):

$$\hat{\boldsymbol{\omega}} = \arg \min_{\bar{\boldsymbol{\omega}}} J(\bar{\boldsymbol{\omega}}) \quad (11)$$

$$J(\bar{\boldsymbol{\omega}}) = \frac{1}{2} \sum_{n=0}^{N-1} \left| y(n) - \bar{\mu} e^{j \sum_{l=0}^1 \bar{\omega}_l n^l} \right|^2. \quad (12)$$

By equating to zero the gradient of $J(\bar{\boldsymbol{\omega}})$, some simple algebra calculations show that the NLS estimates of ω_l , $l = 0, 1$, are asymptotically equivalent to the following estimates (see, e.g., [9], [21]):

$$\hat{\omega}_1 = \arg \max_{\bar{\omega}_1} \frac{1}{N} \left| \sum_{n=0}^{N-1} y(n) e^{-j\bar{\omega}_1 n} \right|^2 \quad (13)$$

$$\hat{\omega}_0 = \text{angle} \left\{ - \sum_{n=0}^{N-1} y(n) e^{-j\hat{\omega}_1 n} \right\}. \quad (14)$$

Note that the NLS estimates of the phase parameters ω_l , $l = 0, 1$, are decoupled from that of the amplitude μ [2]. From (13) and (14), it can be seen that the overall estimation procedure includes two steps. First, a coarse estimate of the frequency offset f_e is determined efficiently by means of the fast Fourier transform algorithm applied on the sequence $y(n)$,

which is generally zero-padded with a sufficiently large number of zeros to achieve the precision provided by the asymptotic CRB ($O(1/N^3)$). Then, a fine frequency offset estimate is obtained by means of interpolation or using a gradient algorithm. Finally, a closed-form estimate of the carrier phase is obtained based on (14), which assumes knowledge of the frequency estimate \hat{f}_e . It is well known that estimator (11) is asymptotically unbiased and consistent [21]. If the distribution of additive noise $u(n)$ is approximated to be circular normal, it turns out that the resulting NLS-estimator is asymptotically efficient, in the sense that it achieves the performance of the ML estimator [2], [9], and [21]. As the simulation experiments illustrate, this approximation holds true for small-order QAM constellations (e.g., quaternary PSK), and the departure from circularity becomes more dominant for larger order QAM constellations.

Following a quite standard procedure (see, e.g., [9], [11], and [21]), one can derive closed-form expressions for the asymptotic variances of estimates $\hat{\omega}_l$, $l = 0, 1$. These calculations are established in the Appendix II and are summarized in the following theorem.

Theorem 1: The asymptotic variances of the NLS estimates $\hat{\omega}_l$, $l = 0, 1$ in (11)–(14) are given by

$$\text{avar}(\hat{\omega}_l) = \frac{\mathcal{B} - \mathcal{D}}{\mathcal{C}^2} \cdot \frac{4l + 2}{N^{2l+1}} \quad (15)$$

$$\mathcal{B} := E\{|y(n)|^2\} = E\{F^2(\rho(n))\} \quad (16)$$

$$\mathcal{D} := |E\{y^2(n)\}| = |E\{F^2(\rho(n))e^{j8\phi(n)}\}| \quad (17)$$

and \mathcal{C} is defined in (9).

Some calculations in Appendix I show that \mathcal{B} , \mathcal{C} , and \mathcal{D} take the following expressions:

$$\mathcal{B} = \int_0^\infty F^2(\rho(n)) \xi_1(\rho(n)) d\rho(n) \quad (18)$$

$$\mathcal{C} = \int_0^\infty F(\rho(n)) \xi_2(\rho(n)) d\rho(n) \quad (19)$$

$$\mathcal{D} = \int_0^\infty F^2(\rho(n)) \xi_3(\rho(n)) d\rho(n) \quad (20)$$

where for $i = 1, 2, 3$, the following relations hold:

$$\begin{aligned} \xi_i(\rho(n)) &:= (-1)^{i-1} \frac{8\rho(n)}{M\sigma_v^2} e^{-(\rho^2(n)/\sigma_v^2)} \\ &\cdot \sum_{l,k \in \mathcal{A}_M} \cos(4(i-1)\varphi_{l,k}) e^{-(\varrho_{l,k}^2/\sigma_v^2)} I_{4(i-1)} \left(\frac{2\rho(n)\varrho_{l,k}}{\sigma_v^2} \right) \end{aligned} \quad (21)$$

and $\varphi_{l,k} := \psi_{\max\{l,k\}, \min\{l,k\}}$.

$$f(\rho(n), \phi(n)) = \frac{\rho(n)}{M\pi\sigma_v^2} \sum_{(l,k) \in \mathcal{A}_M} \sum_{m=0}^3 e^{-(1/\sigma_v^2)[\rho^2(n) + \varrho_{l,k}^2]} e^{(2\rho(n)\varrho_{l,k})/\sigma_v^2} \cos[\phi(n) - \psi_{l,k} - (m\pi/2) - \eta(n)] \quad (5)$$

$$f(\rho(n)) = \int_{-\pi}^{\pi} f(\rho(n), \phi(n)) d\phi(n) = \frac{8\rho(n)}{M\sigma_v^2} \sum_{(l,k) \in \mathcal{A}_M} e^{-(\rho^2(n) + \varrho_{l,k}^2)/\sigma_v^2} I_0 \left(\frac{2\rho(n)\varrho_{l,k}}{\sigma_v^2} \right) \quad (6)$$

From the above expressions, one can observe that the asymptotic variances of $\hat{\omega}_l$, $l = 0, 1$, are independent of the unknown phase parameters θ and f_e . It is of interest to compare the asymptotic variances (15) with the CRB. In [18], the CRBs for carrier phase and frequency offset estimates are derived for fully QAM-modulated carriers, and with the notations adopted so far admit the following expression for large N :

$$\text{CRB}(\hat{\omega}_l) = \text{CRB}_{\text{CW}}(\hat{\omega}_l) \cdot R(\sigma_v^2) = \frac{(4l+2)\sigma_v^2}{N^{2l+1}} \cdot R(\sigma_v^2) \quad (22)$$

where CRB_{CW} corresponds to the CRB for an unmodulated carrier wave, and $R(\sigma_v^2)$ denotes the constellation-dependent ratio of the true CRB to CRB_{CW} , which can be evaluated by means of numerical integration or Monte Carlo evaluations [18]. Based on (15) and (22), one can observe that the asymptotic variances $\text{avar}(\hat{\omega}_l)$ of the NLS estimates $\hat{\omega}_l$, $l = 0, 1$, decay at the same rate as the CRB, i.e., $O(1/N^{2l+1})$.

In the absence of frequency offset (f_e), the proposed NLS estimator (11) reduces to the phase estimator

$$\hat{\theta} = \frac{1}{4} \text{angle} \left\{ - \sum_{n=0}^{N-1} y(n) \right\} \quad (23)$$

whose asymptotic variance is one quarter of that corresponding to the case of joint phase and frequency offset estimation [18], and is given by

$$\text{avar}(\hat{\theta}) = \frac{\mathcal{B} - \mathcal{D}}{32N\mathcal{C}^2}. \quad (24)$$

Next, we determine the optimal ‘‘matched’’ nonlinearity $F(\cdot)$ which minimizes the asymptotic variance $\text{avar}(\hat{\omega}_l)$ (15). Since in (15) only the terms \mathcal{B} , \mathcal{C} , \mathcal{D} depend on $F(\cdot)$, finding an optimal $F(\cdot)$ resorts to solving the optimization problem

$$F_{\min}(\rho(n)) = \arg \min_{F(\cdot)} \frac{\mathcal{B} - \mathcal{D}}{\mathcal{C}^2}.$$

Based on (9), (16), and (17), the optimum nonlinearity F_{\min} is obtained by using Cauchy–Schwarz’ inequality and is given by the following theorem.

Theorem 2: The optimal ‘‘matched’’ nonlinearity $F_{\min}(\cdot)$ that minimizes the asymptotic variances of the proposed family of NLS estimators (11) is given by

$$F_{\min}(\rho(n)) = \lambda \frac{\xi_2(\rho(n))}{\xi_1(\rho(n)) - \xi_3(\rho(n))} \quad (25)$$

where λ is an arbitrary nonzero constant selected such that $F_{\min}(\cdot)$ is nonnegative.

Plugging (25) back into (18)–(20), and substituting these values into (15), the asymptotic variances corresponding to the optimal matched estimates $\hat{\omega}_l$, $l = 0, 1$, can be expressed as

$$\text{avar}_{\min}(\hat{\omega}_l) = \frac{4l+2}{N^{2l+1}} \cdot \frac{1}{\int_0^\infty \frac{\xi_2^2(\rho(n))}{\xi_1(\rho(n)) - \xi_3(\rho(n))} d\rho(n)}. \quad (26)$$

B. Monomial Nonlinear Estimators

The conventional V&V-like nonlinearities rely on the monomial transformations $F_k(\rho(n)) = \rho^k(n)$, $k = 0, \dots, 4$, and ex-

hibit computational efficiency and simplicity when compared with the optimal matched estimator. In this subsection, we derive closed-form expressions for the asymptotic variances of this class of monomial phase and frequency offset estimators. Define the class of processes $y_k(n)$, $n = 0, \dots, N$

$$y_k(n) = \rho^k(n) e^{j4\phi(n)}, \quad k = 0, \dots, 4 \quad (27)$$

and the zero-mean processes: $u_k(n) := y_k(n) - E\{y_k(n)\}$, $k = 0, \dots, 4$. As before, it turns out that $E\{y_k(n)\}$ is a constant amplitude harmonic, and hence, $y_k(n) = E\{y_k(n)\} + u_k(n)$ can be interpreted as a constant amplitude harmonic embedded in additive noise. As a special case of (11), we introduce the following class of monomial NLS estimators:

$$\hat{\omega}^{(k)} = \arg \min_{\bar{\omega}^{(k)}} \frac{1}{2} \sum_{n=0}^{N-1} \left| y_k(n) - \bar{\mu}^{(k)} e^{j \sum_{l=0}^1 \bar{\omega}_l^{(k)} n^l} \right|^2 \quad (28)$$

whose asymptotic variances for $\hat{\omega}_l^{(k)}$, $l = 0, 1$ are provided by the following theorem.

Theorem 3: The asymptotic variances of the NLS estimates $\hat{\omega}_l^{(k)}$, $l = 0, 1$, in (28), are given by

$$\begin{aligned} \text{avar}(\hat{\omega}_l^{(k)}) &= \frac{\mathcal{B}_k - \mathcal{D}_k}{\mathcal{C}_k^2} \cdot \frac{4l+2}{N^{2l+1}} \\ \mathcal{B}_k &:= E\{|y_k(n)|^2\} = E\{\rho^{2k}(n)\} \\ \mathcal{C}_k &:= |E\{y_k(n)\}| = |E\{\rho^k(n) e^{j4\phi(n)}\}| \\ \mathcal{D}_k &:= |E\{y_k^2(n)\}| = |E\{\rho^{2k}(n) e^{j8\phi(n)}\}|. \end{aligned} \quad (29)$$

Exploiting (6) and [10, eq. (6.643.4)], the following closed-form expression for \mathcal{B}_k can be derived:

$$\mathcal{B}_k = \frac{4\sigma_v^{2k}}{M} \sum_{q=0}^k \binom{k}{q}^2 q! \sum_{l,p \in \mathcal{A}_M} \left(\frac{\varrho_{l,p}^2}{\sigma_v^2} \right)^{k-q}. \quad (30)$$

From Appendix III, \mathcal{C}_k and \mathcal{D}_k , $k = 0, \dots, 4$ can be expressed in terms of confluent hypergeometric function $\Phi(\cdot, \cdot, \cdot)$ as follows:

$$\begin{aligned} \mathcal{C}_k &= - \frac{4\sigma_v^{k-4} \Gamma(\frac{k}{2} + 3)}{M \Gamma(5)} \\ &\cdot \sum_{(l,p) \in \mathcal{A}_M} \cos(4\varphi_{l,p}) e^{-\varrho_{l,p}^2/\sigma_v^2} \varrho_{l,p}^4 \Phi\left(\frac{k}{2} + 3, 5, \frac{\varrho_{l,p}^2}{\sigma_v^2}\right) \end{aligned} \quad (31)$$

$$\begin{aligned} \mathcal{D}_k &= \frac{4\sigma_v^{2k-8} \Gamma(k+5)}{M \Gamma(9)} \\ &\cdot \sum_{(l,p) \in \mathcal{A}_M} \cos(8\varphi_{l,p}) e^{-\varrho_{l,p}^2/\sigma_v^2} \varrho_{l,p}^8 \Phi\left(k+5, 9, \frac{\varrho_{l,p}^2}{\sigma_v^2}\right). \end{aligned} \quad (32)$$

It should be pointed out that when k is even (M is usually a power of two), following a similar approach to that presented in [22] or the formula [1, eq. (13.5.1)], one can obtain a slightly

more compact expression for the confluent hypergeometric function in (31)

$$\begin{aligned} \mathcal{C}_k &= -\frac{4}{M} \sum_{(l,p) \in \mathcal{A}_M} \cos(4\varphi_{l,p}) \mathcal{H}\left(\frac{k}{2}, 2, \frac{\varrho_{l,p}^2}{\sigma_v^2}\right), \quad \text{if } k=0, 2 \\ \mathcal{C}_k &= -\frac{4}{M} \sum_{(l,p) \in \mathcal{A}_M} \cos(4\varphi_{l,p}) \varrho_{l,p}^4, \quad \text{if } k=4 \\ \mathcal{H}(s, t, \gamma) &:= \left(\frac{\sigma_v^2}{2}\right)^t \left[\gamma^t \sum_{p=0}^{s+t} p! \binom{s+t}{p} \binom{s-t+p-1}{p} \left(\frac{-2}{\gamma}\right)^p \right. \\ &\quad \left. + (-1)^{s+t+1} 2^t e^{-(\gamma/2)} \left(\frac{2}{\gamma}\right)^{t+1} \right. \\ &\quad \left. \cdot \sum_{p=0}^{s-t-1} \binom{s+t+p}{p} \frac{(s+t)!}{(s-t-p-1)!} \left(\frac{2}{\gamma}\right)^p \right]. \end{aligned}$$

Similarly

$$\begin{aligned} \mathcal{D}_k &= \frac{4}{M} \sum_{(l,p) \in \mathcal{A}_M} \cos(8\varphi_{l,p}) \mathcal{H}\left(k, 4, \frac{\varrho_{l,p}^2}{\sigma_v^2}\right), \quad \text{if } k=0, 1, 2, 3 \\ \mathcal{D}_k &= \frac{4}{M} \sum_{(l,p) \in \mathcal{A}_M} \cos(8\varphi_{l,p}) \varrho_{l,p}^8, \quad \text{if } k=4. \end{aligned}$$

Plugging (30), (31), and (32) back into (29), closed-form expressions for the asymptotic variances $\text{avar}(\hat{\omega}_l^{(k)})$ for $k=0, \dots, 4$ and $l=0, 1$ are obtained. Note that when $k=4$, the phase estimator (23) is just the standard fourth-power estimator [3], [12, pp. 281–282], and [15], and (24) coincides with the expression established earlier in [20, eq. (13)].

IV. EXTENSION TO CROSS-QAM CONSTELLATIONS

Following a similar approach to the one presented above, one can develop an optimal matched joint carrier phase and frequency offset estimator for general cross-QAM modulations (i.e., with sizes $M = 2^{2m+1}$, $m = 2, 3, \dots$). Observe that for general cross-QAM constellations, $w(n)$ takes a value from the set $(1/r_w)\{\pm(1+2l) \pm j(1+2k), (l, k) \in \mathcal{A}_M\}$, with $\mathcal{A}_M := \{(0, 1, \dots, 3 \cdot 2^{m-2} - 1)^2 - (2^{m-1}, \dots, 3 \cdot 2^{m-2} - 1)^2\}$ and r_w an energy normalization constant. Therefore, we can still express the joint and marginal pdf of $\rho(n)$ and $\phi(n)$ as in (5) and (6). Similarly, to the derivations presented in Section III, by considering the process $y(n)$ [see (3)], it follows that $y(n)$ can be interpreted as the sum (10). Therefore, it is not difficult to find that all the estimators proposed for square-QAM modulations can be applied to cross-QAM constellations, and all the expressions for the asymptotic variances still hold true without any change. The constants $\mathcal{B}_k, \mathcal{C}_k, \mathcal{D}_k$ are constellation-dependent and their values should be computed accordingly. Due to space limitations, we will not present any detailed derivations.

In Figs. 1–3, we evaluate the theoretical asymptotic variances of the proposed optimal matched and monomial estimators versus SNR. Fig. 1 depicts the performance loss of the asymptotic variances (26) and (29) with respect to the CRB (22) (i.e., $-10 \log_{10}[\text{avar}(\hat{\omega}_l)/\text{CRB}(\hat{\omega}_l)]$) for 4-QAM modulation. It

turns out that the proposed optimal estimator approaches the CRB in low and high SNR ranges, and in almost the entire SNR region of interest, the optimal nonlinearity $F_{\min}(\rho(n))$ can be approximated without much loss in performance by $\rho^2(n)$. However, the same conclusion can not be drawn for larger order QAM constellations. Assuming the number of samples $N = 500$, Figs. 2 and 3 illustrate the theoretical asymptotic variances for 16-QAM (square) and 32-QAM (cross), respectively. Since the difference between the asymptotic variances of $\hat{\theta}$ and \hat{f}_e is just a constant for a given SNR, only the variance of $\hat{\theta}(24)$ is plotted. From Figs. 2 and 3, one can observe that at low SNRs, both the optimal estimator and the fourth-power estimator achieve CRB, which means that at very low SNRs, the classic fourth-power estimator is always the best choice. This is not a surprising result since the fourth-power estimator is simply a low-SNR approximation of the ML estimator [15]. However, in the more practical regime of medium and high SNRs, the optimum nonlinear estimator provides a significant improvement over the class of monomial estimators while the latter exhibits the error floor due to its self-induced noise [15], [18].

V. IMPLEMENTATION OF THE OPTIMAL ESTIMATOR

The results shown in Figs. 2 and 3 illustrate the good property of the optimal nonlinearity (25) for higher order QAM modulations at medium and high SNR ranges. As can be observed from (21) and (25), $F_{\min}(\rho(n))$ is a function that depends on the SNR and presents high implementation complexity, which makes the optimal estimator impractical. Fortunately, computer simulations indicate that the sensitivity of the optimal estimator to SNR is limited in medium and high SNR ranges. By considering approximations of (25), we propose next computationally efficient SNR-independent estimators, which will be referred to as approximate (APP)-estimators.

We select 16-QAM as an example to illustrate the derivation of the constellation-dependent APP estimator. Fig. 4(a) plots the optimal nonlinearity (25) versus the magnitude ρ of the received data at SNR = 20 dB for 16-QAM modulation, while Fig. 4(b) depicts the optimal nonlinearity (25) for a set of varying SNRs. The curve presented in Fig. 4(a) suggests that for 16-QAM a good design for the APP estimator is a piecewise linear approximation of the following form:

$$F_{\text{APP}_{16}}(\rho(n)) = \begin{cases} 122.2733\rho(n), & \text{if } \rho(n) \leq 0.7 \\ 331.885\rho(n) - 30.4524, & \text{if } \rho(n) \geq 1.2 \\ 0, & \text{elsewhere.} \end{cases} \quad (33)$$

Similarly for 32-QAM and 64-QAM, since the optimal nonlinearity (25) appears to be well modeled by piecewise linear approximations, we can obtain the APP estimators

$$F_{\text{APP}_{32}}(\rho(n)) = \begin{cases} 206.9958\rho(n), & \text{if } \rho(n) \leq 0.5 \\ 608.4586\rho(n) + 2.2689, & \text{if } \rho \in [0.84, 1.02] \\ 0, & \text{elsewhere} \end{cases}$$

$$F_{\text{APP}_{64}}(\rho(n)) = \begin{cases} 106.4159\rho(n), & \text{if } \rho(n) \leq 0.34 \\ 321.2425\rho(n), & \text{if } \rho \in [0.59, 0.69] \\ 717\rho(n), & \text{if } \rho(n) \geq 1.44 \\ 0, & \text{elsewhere} \end{cases}$$

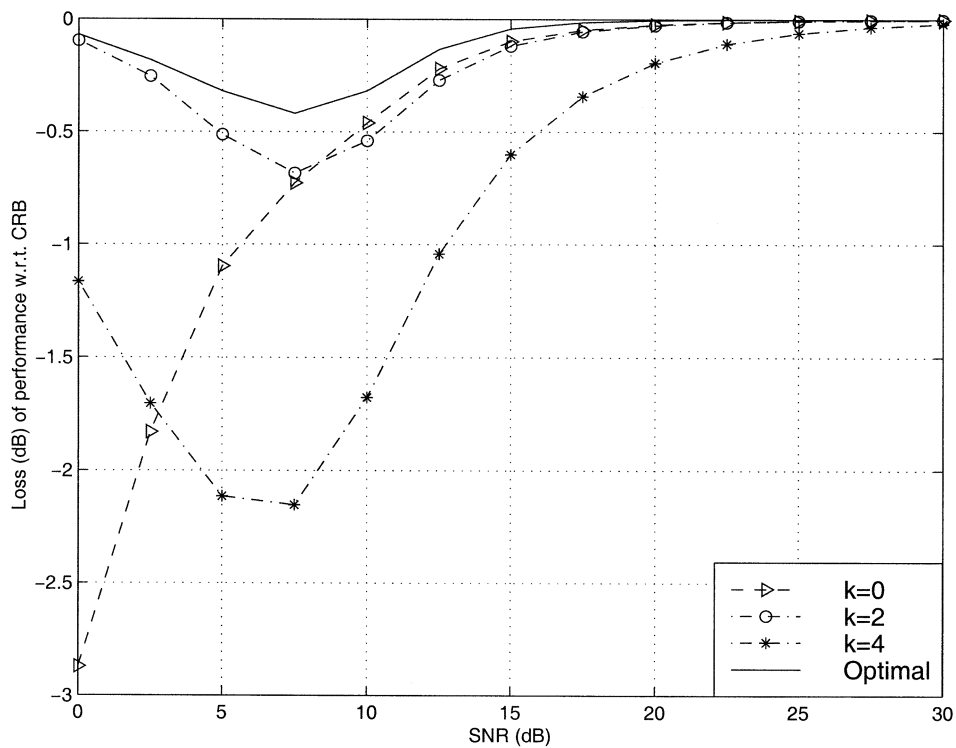


Fig. 1. Performance loss with respect to the CRB versus SNR (4-QAM constellation).

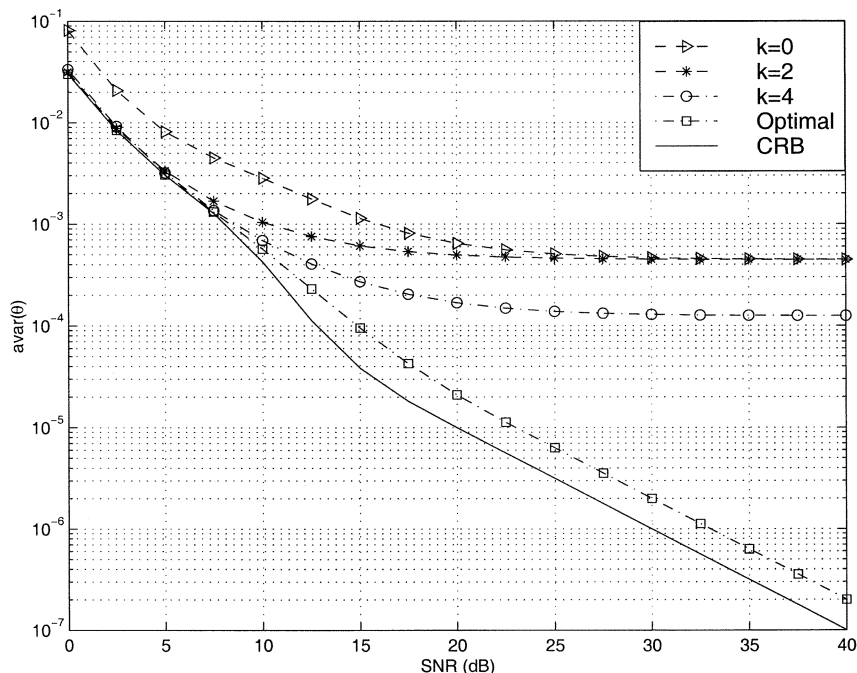


Fig. 2. Theoretical bounds of $\hat{\theta}$ versus SNR (16-QAM constellation).

respectively. Since $F_{APP}(\cdot)$ is constellation-dependent, we will not present the detailed expressions of F_{APP} for other QAM modulations in this paper. The APP nonlinearities for general QAM constellations can be obtained in a similar way. It is interesting to observe that $F_{APP_{16}}(33)$ is quite similar to the nonlinearity introduced in the Morelli *et al.* estimator [V&V algorithm

with selection (V&V-SEL)] [13], which takes the following expression:

$$F_{V\&V-SEL}(\rho(n)) = \begin{cases} 0.4472\rho(n), & \text{if } \rho(n) \leq 0.7236 \\ 1.3416\rho(n), & \text{if } \rho(n) \geq 1.1708 \\ 0, & \text{elsewhere.} \end{cases}$$

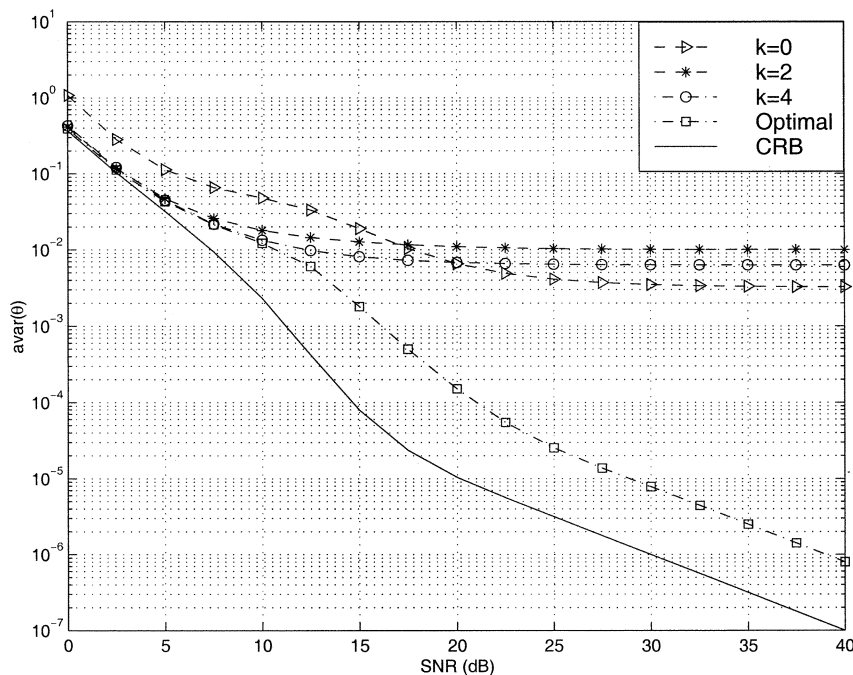


Fig. 3. Theoretical bounds of $\hat{\theta}$ versus SNR (32-QAM constellation).

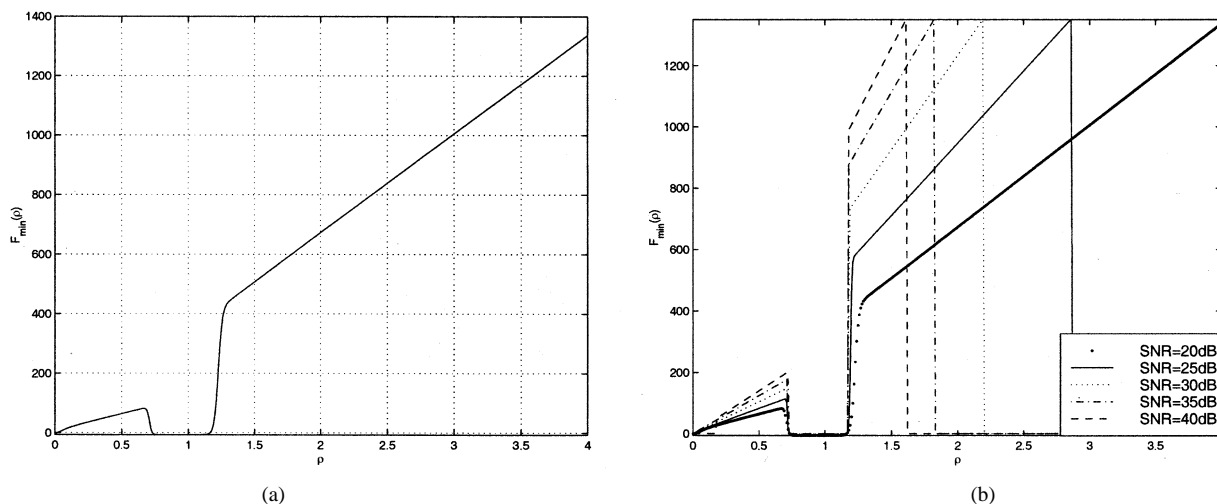


Fig. 4. (a) F_{\min} versus ρ (16-QAM constellation at SNR = 20 dB). (b) F_{\min} versus ρ (16-QAM constellation at varying SNRs).

Careful examination of the expressions of APP nonlinearities illustrates that the intrinsic principle of APP estimators is to emphasize the weight of the points located on the diagonals of the signal constellation, and discard all the off-diagonal points. It appears also that only a subset of the points located on the diagonals is selected. This principle was implicitly exploited by V&V-SEL estimator [13] for 16-QAM, and by Sari and Moridi for 16-QAM and 64-QAM under quite different circumstances [19].

In the next section, we will present simulation experiments to corroborate the theoretical performance analysis and to illustrate the performance of the proposed optimal estimators for both square- and cross-QAM constellations.

VI. SIMULATION EXPERIMENTS

In this section, we study thoroughly the performance of estimators (11), (23), and (28) using computer simulations. The experimental mean-square error (MSE) results of the proposed estimators will be compared with the theoretical asymptotic bounds and the CRB. The impact of the nonlinearity $F(\cdot)$ on SER is also assessed. The additive noise is generated as zero-mean Gaussian white noise, the number of samples is assumed $N = 500$, and the experimental results are obtained by performing a number of $MC = 1000$ Monte Carlo trials except in Figs. 5–8, where we use a larger number $MC = 100000$ to ensure accuracy. Unless otherwise noted, the carrier phase $\theta = 0.2$ and frequency offset $F_e T = 0.05$.

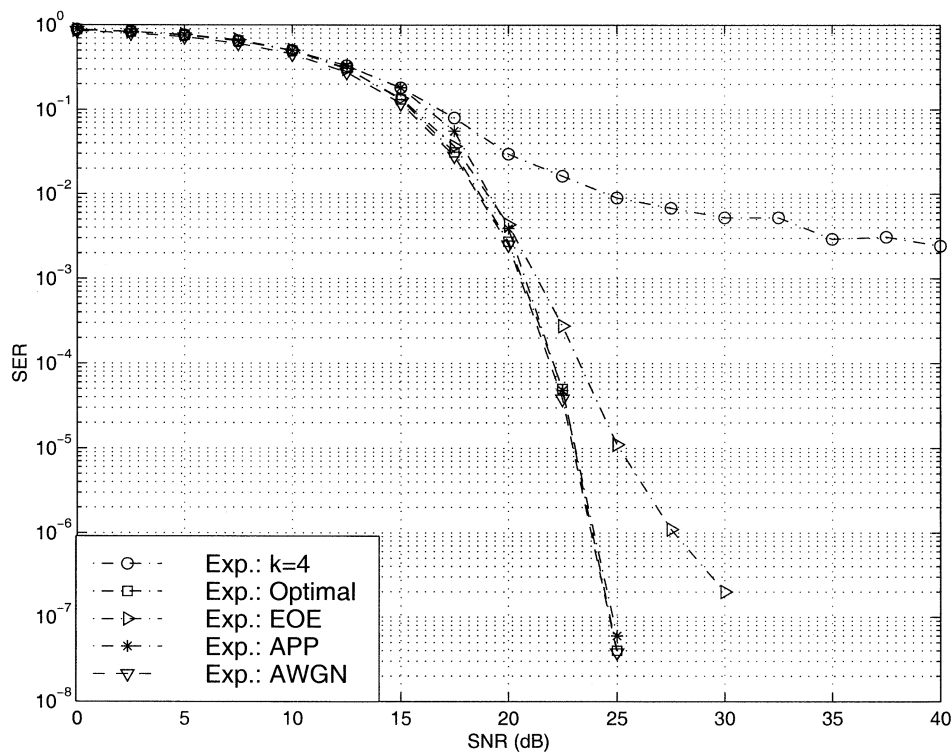


Fig. 5. SER curves versus SNR (32-QAM constellation).

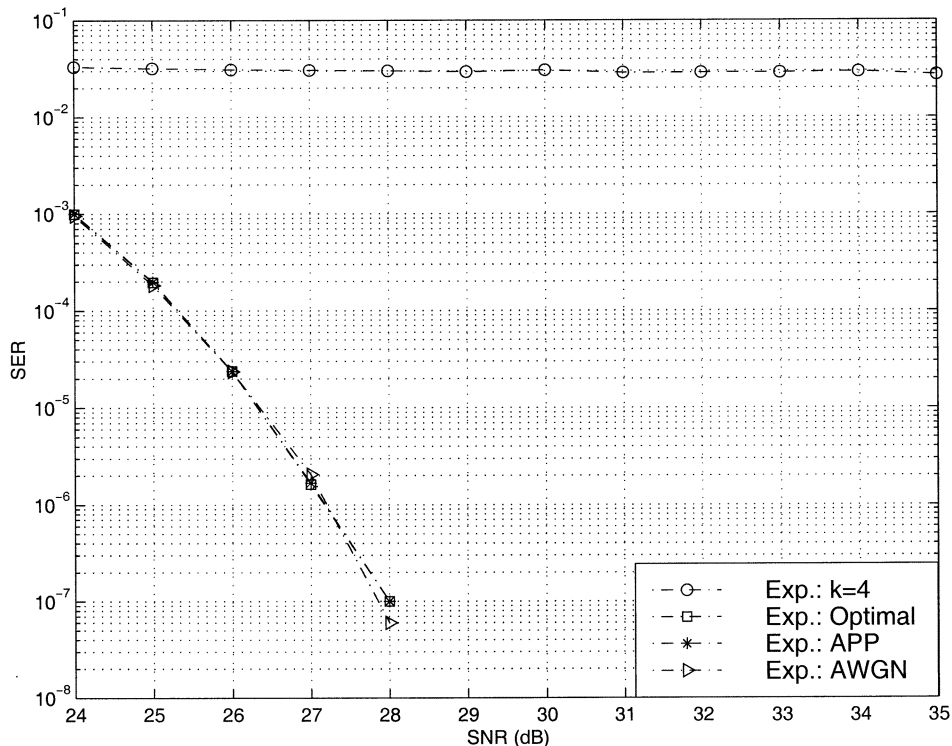


Fig. 6. SER curves versus SNR (64-QAM constellation).

A. Experiment 1—Comparison of the MSE of the Proposed Estimators With the Theoretical Bounds Versus SNR

This experiment compares the theoretical (The.) bounds with the experimental (Exp.) MSEs of the proposed estimators for 16-QAM (Figs. 9 and 10) and 32-QAM (Fig. 11) assuming

no frequency offset. In Figs. 9 and 10, the performance of V&V-SEL estimator [13] is illustrated, too, while in Fig. 11, we also plot the MSE-result of the eighth-order statistics based phase estimator (EOE) proposed for cross QAM in [4]. These figures show that for medium and high SNRs, the experimental results of the optimal estimator and the fourth-power estimator

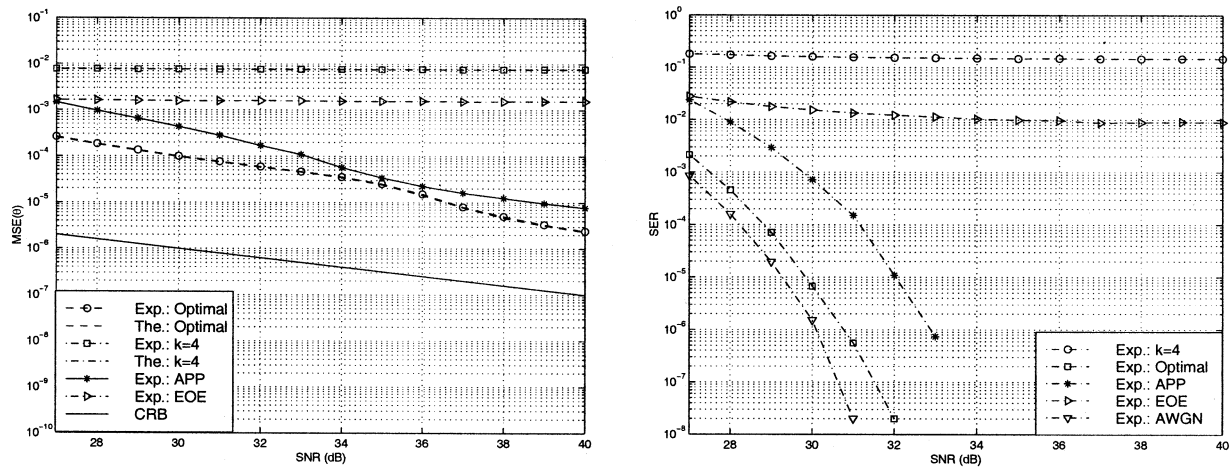


Fig. 7. MSE and SER versus SNR (128-QAM constellation).

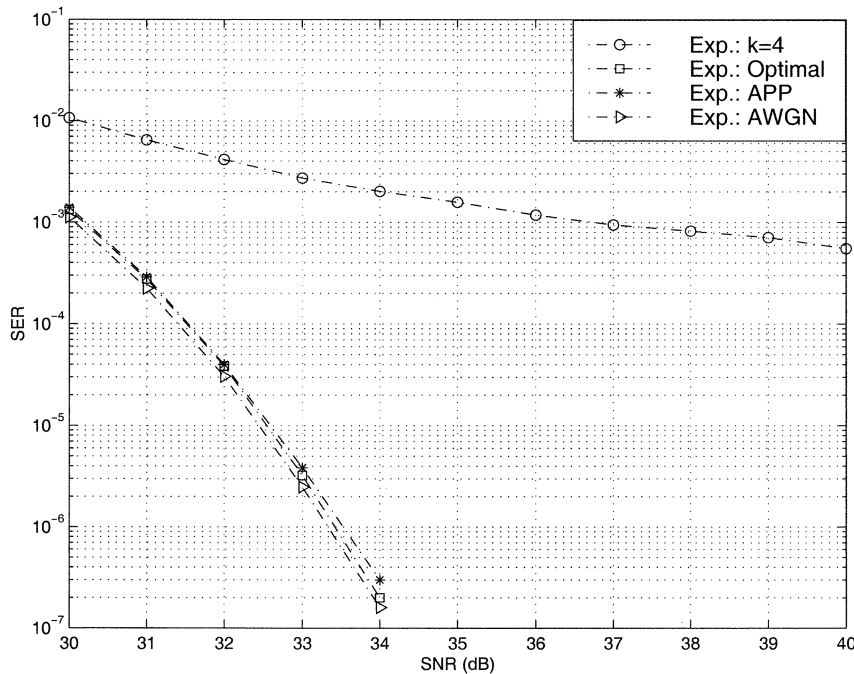


Fig. 8. SER curves versus SNR (256-QAM constellation).

are well predicted by the asymptotic bounds derived in this paper. Note that at low SNR (0 dB), the MSE of the phase estimator (23) asymptotically converges toward the constant value $\pi^2/48$, which represents the variance of a uniformly distributed phase estimate over the range $[-\pi/4, \pi/4]$ [18], [22]. From Figs. 9 and 10, we can observe that for 16-QAM, the performance of the optimal estimator and the V&V-SEL estimator is essentially identical, and both of them outperform significantly the standard fourth-power estimator in the medium and high SNR ranges, and are very close to CRB. In the case of cross-QAM constellations, the proposed optimal phase estimator provides considerable improvement over the fourth-power estimator and EOE.

B. Experiment 2—Impact of the Nonlinearity on SER

In Figs. 5 and 12, we show the SER performance of the carrier synchronizers exploiting different nonlinearities and

QAM modulations. Because the choice of nonlinearity $F(\cdot)$ is the same for both carrier phase and frequency offset estimators, for simplicity we only concentrate on the carrier phase estimator assuming the absence of frequency offset. Figs. 5 and 12 compare the performance of the proposed optimal and APP estimators with that of the classic fourth-power estimator, V&V-SEL estimator, and EOE for 16-QAM with $\theta = 0.75$ and 32-QAM with $\theta = 0.2$, respectively. To show the superior performance of the optimal estimator, we also plot as a lower bound the SER curves in the case of perfect carrier recovery, i.e., in the case when the transmitted symbols are only corrupted by additive white Gaussian noise (AWGN). Figs. 5 and 12 indicate that the proposed optimal estimator approaches closely this lower bound and improves significantly the performance of the conventional fourth-power estimator and EOE for medium and high SNRs. We can also observe that APP is a satisfying realizable alternative to the optimal estimator.

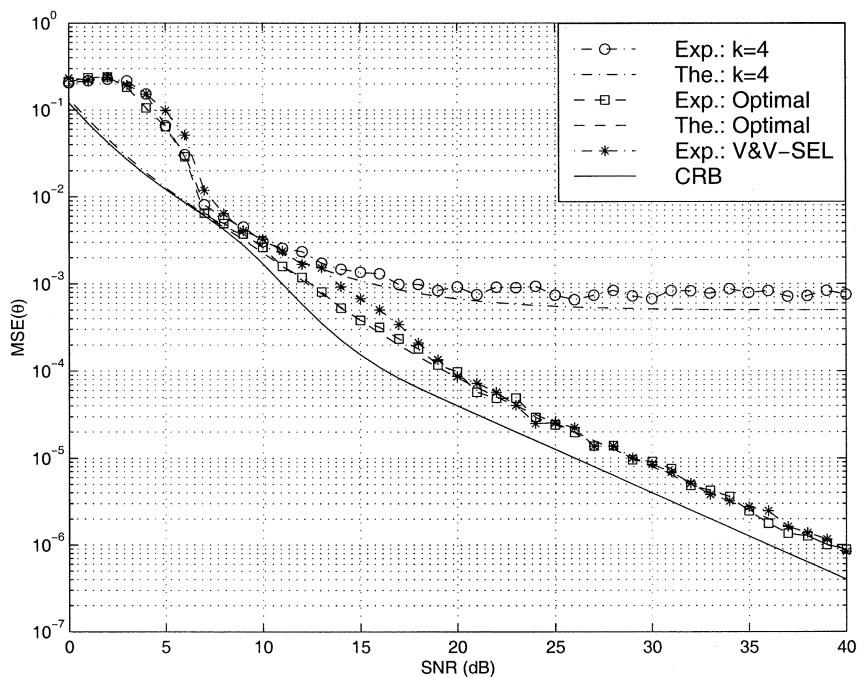


Fig. 9. Comparison of MSEs of $\hat{\theta}$ versus SNR (16-QAM constellation).

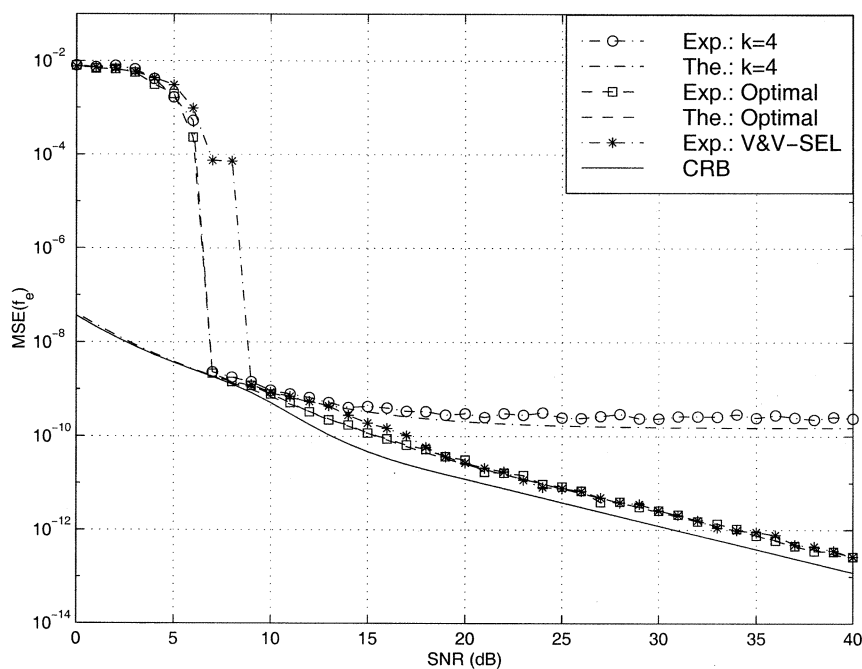


Fig. 10. Comparison of MSEs of \hat{f}_e versus SNR (16-QAM constellation).

C. Experiment 3—Performance of the Proposed Estimators in the Case of Higher Order QAM Modulations

Figs. 6–8 illustrate the performance of the optimal estimator and APP for larger order QAM modulations (64-QAM with $\theta = 0.75$, 128-QAM, and 256-QAM, respectively) compared with the existing methods. Since higher order QAM modulations often operate at larger SNRs, we pay special attention to the medium and high SNRs, where the SER is in the range $SER \leq 10^{-3}$. These figures show again the merit of the pro-

posed optimal estimator and APP, and justify again our derivation of the asymptotic variance.

VII. CONCLUSION

In this paper, we have introduced and analyzed a family of blind feedforward joint carrier phase and frequency offset estimators for general QAM modulations. Based on a generalization of the V&V algorithm, a matched nonlinear estimator together with a class of monomial nonlinear estimators were introduced and their performance established in closed-form

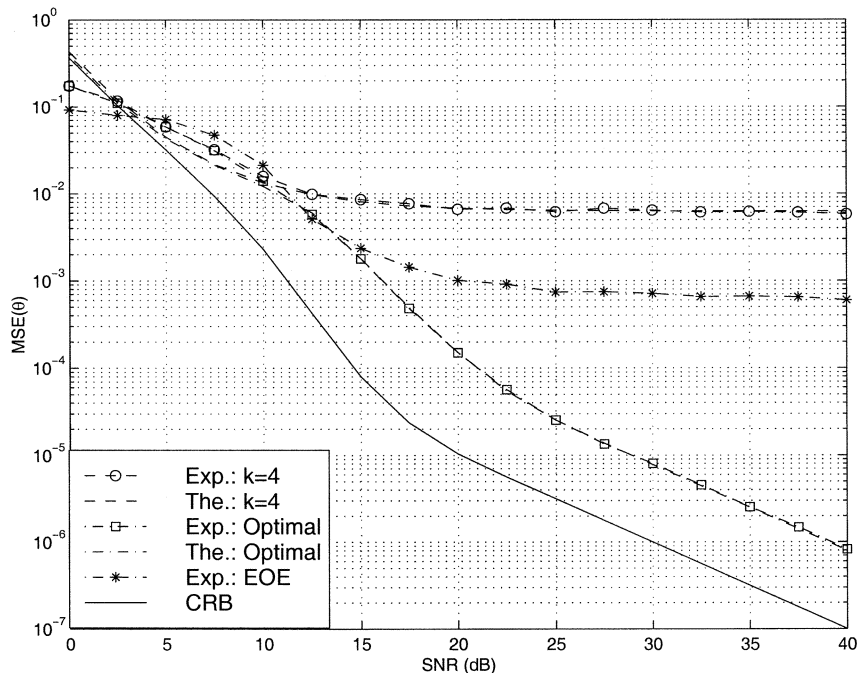


Fig. 11. Comparison of MSEs of $\hat{\theta}$ versus SNR (32-QAM constellation).

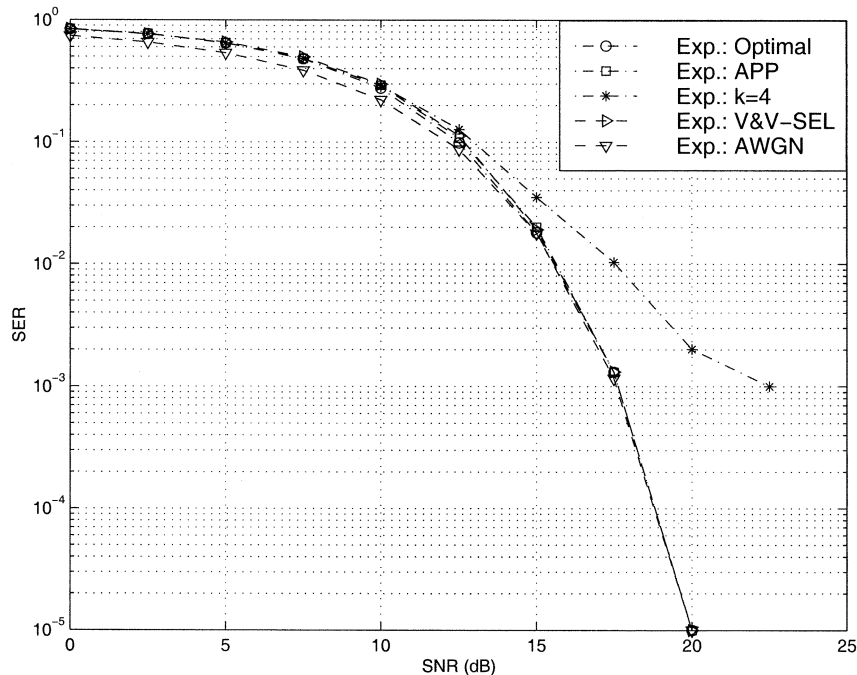


Fig. 12. SER curves versus SNR (16-QAM constellation).

expressions. A framework for designing computationally efficient approximations of the proposed optimal estimator without incurring much performance loss, is also proposed. The proposed (approximate) optimal estimator exhibits better performance when compared with the existing methods. Simulation results indicate the merit of the performance analysis presented in this paper. In a future paper, we will analyze the performance of a generalized NLS estimator that exploits the

information provided by the two spectral lines present in the process: $y(n) := F_1(\rho(n))e^{j4\phi(n)} + F_2(\rho(n))e^{j8\phi(n)}$, where $F_1(\cdot)$ and $F_2(\cdot)$ are two arbitrary nonlinearities. It appears that for square QAM or small-order QAM there is not too much room for improvement, a fact that is corroborated by the SER curves depicted in Figs. 5–8 and 12. However, for larger order cross QAM, the exploitation of additional harmonics (lines) may provide some performance gains.

APPENDIX I
DERIVATION OF (18) AND (19)

Using (5), we can express $E\{y(n)\}$ as (34), at the bottom of the page, where in deriving the third equality, we made use of the definition of $I_4(\cdot)$ [1, eq. (9.6.19)]. For a fixed pair (l, k) and $l > k$, $\psi_{k,l} = -\psi_{l,k} + \pi/2$, so $\exp(4\psi_{k,l}) = \exp(-4\psi_{l,k})$. After defining $\varphi_{l,k} := \psi_{\max\{l,k\}, \min\{l,k\}}$ and

$$\xi_2(\rho(n)) := -\frac{8\rho(n)}{M\sigma_v^2} e^{-(\rho^2(n)/\sigma_v^2)} \cdot \sum_{(l,k) \in \mathcal{A}_M} \cos(4\varphi_{l,k}) e^{-(\varrho_{l,k}^2/\sigma_v^2)} I_4\left(\frac{2\rho(n)\varrho_{l,k}}{\sigma_v^2}\right)$$

we obtain from (34)

$$\mathcal{C} := |E\{y(n)\}| = \int_0^\infty F(\rho(n)) \xi_2(\rho(n)) d\rho(n)$$

which is (19). Equations (18) and (20) can be obtained using a similar procedure.

APPENDIX II
PROOF OF THEOREM 1

In order to establish Theorem 1, let us first study the second-order statistics of additive noise $u(n)$. From (10), $u(n)$ can be expressed as

$$u(n) := y(n) - E\{y(n)\} \\ = F(\rho(n))e^{j4\phi(n)} - E\{F(\rho(n))e^{j4\phi(n)}\}.$$

Define the second-order covariance and relation functions of $u(n)$ as

$$r_u(n; \tau) \\ := E\{u^*(n)u(n+\tau)\}$$

$$= E\left\{F(\rho(n))e^{-j4\phi(n)}F(\rho(n+\tau))e^{j4\phi(n+\tau)}\right\} \\ - E\left\{F(\rho(n))e^{-j4\phi(n)}\right\}E\left\{F(\rho(n+\tau))e^{j4\phi(n+\tau)}\right\} \\ \tilde{r}_u(n; \tau) \\ := E\{u(n)u(n+\tau)\} \\ = E\left\{F(\rho(n))e^{j4\phi(n)}F(\rho(n+\tau))e^{j4\phi(n+\tau)}\right\} \\ - E\left\{F(\rho(n))e^{j4\phi(n)}\right\}E\left\{F(\rho(n+\tau))e^{j4\phi(n+\tau)}\right\}$$

respectively. Due to (7), it turns out that $r_u(n; \tau)$ and $\tilde{r}_u(n; \tau)$ are both equal to zero if $\tau \neq 0$. Hence, we obtain from (9), (16), and (17) the following relations:

$$r_u(n; \tau) = \left[E\{F^2(\rho(n))\} - \left| E\{F(\rho(n))e^{j4\phi(n)}\} \right|^2 \right] \delta(\tau) \\ = (\mathcal{B} - \mathcal{C}^2) \delta(\tau) \quad (35)$$

$$\tilde{r}_u(n; \tau) = \left[E\{F^2(\rho(n))e^{j8\phi(n)}\} - E^2\{F(\rho(n))e^{j4\phi(n)}\} \right] \\ \cdot \delta(\tau) = (\mathcal{D} - \mathcal{C}^2)e^{j8\eta(n)} \delta(\tau) \quad (36)$$

where $\delta(\cdot)$ stands for the Kronecker's delta.

Next, we begin the derivation of Theorem 1. Since $\mu := -\mathcal{C}$, for simplicity, we replace μ by \mathcal{C} in the cost function (12). Considering the Taylor series expansion of $\hat{\mathcal{C}} \exp(j \sum_{l=0}^1 \hat{\omega}_l n^l)$ in the neighborhood of the true value $[\mathcal{C} \ \omega_0 \ \omega_1]^T$, we can write

$$\hat{\mathcal{C}} e^{j \sum_{l=0}^1 \hat{\omega}_l n^l} = \mathcal{C} e^{j \sum_{l=0}^1 \omega_l n^l} + (\hat{\mathcal{C}} - \mathcal{C}) e^{j \sum_{l=0}^1 \omega_l n^l} \\ + j \sum_{k=0}^1 n^k (\hat{\omega}_k - \omega_k) \mathcal{C} e^{j \sum_{l=0}^1 \omega_l n^l} + \text{rem}$$

where rem stands for the high-order remainder terms which asymptotically as $N \rightarrow \infty$ can be neglected. Thus, we can approximate (12), as shown in the equation at the bottom of the page. Setting the derivatives of $J(\hat{\omega})$ with respect to $\hat{\omega}$ to 0, we

$$E\{y(n)\} \\ = E\{F(\rho(n))e^{j4\phi(n)}\} \\ = \frac{1}{M\pi\sigma_v^2} \sum_{(l,k) \in \mathcal{A}_M} \sum_{m=0}^3 \int_0^\infty \rho(n) F(\rho(n)) e^{-(\rho^2(n) + \varrho_{l,k}^2/\sigma_v^2)} \int_{-\pi}^{\pi} e^{j4\phi(n)} e^{(2\rho(n)\varrho_{l,k}/\sigma_v^2) \cos[\phi(n) - \psi_{l,k} - (m\pi/2) - \eta(n)]} d\phi(n) d\rho(n) \\ = e^{j4\eta(n)} \frac{2}{M\sigma_v^2} \sum_{(l,k) \in \mathcal{A}_M} \sum_{m=0}^3 e^{j2\pi m} e^{j4\psi_{l,k}} \int_0^\infty \rho(n) F(\rho(n)) e^{-(\rho^2(n) + \varrho_{l,k}^2/\sigma_v^2)} I_4\left(\frac{2\rho(n)\varrho_{l,k}}{\sigma_v^2}\right) d\rho(n) \\ = e^{j4\eta(n)} \frac{8}{M\sigma_v^2} \sum_{(l,k) \in \mathcal{A}_M} e^{j4\psi_{l,k}} \int_0^\infty \rho(n) F(\rho(n)) e^{-(\rho^2(n) + \varrho_{l,k}^2/\sigma_v^2)} I_4\left(\frac{2\rho(n)\varrho_{l,k}}{\sigma_v^2}\right) d\rho(n) \quad (34)$$

$$J(\hat{\omega}) \doteq \frac{1}{2} \sum_{n=0}^{N-1} \left| y(n) - \mathcal{C} e^{j \sum_{l=0}^1 \omega_l n^l} - (\hat{\mathcal{C}} - \mathcal{C}) e^{j \sum_{l=0}^1 \omega_l n^l} - j \sum_{k=0}^1 n^k (\hat{\omega}_k - \omega_k) \mathcal{C} e^{j \sum_{l=0}^1 \omega_l n^l} \right|^2$$

obtain the first equation at the bottom of the page.² We normalize the above equations by $N^{1/2}$ and $N^{k+1/2}$, $k = 0, 1$, respectively, and obtain that asymptotically (as $N \rightarrow \infty$) the relations hold, as shown in (37) and (38), at the bottom of the page, where in deriving the last equality, we made use of the well-known limit [11]

$$\lim_{N \rightarrow \infty} \frac{1}{N} \sum_{n=0}^{N-1} \left(\frac{n}{N}\right)^k = \frac{1}{k+1}.$$

Next, we express (37) and (38) in the matrix compact form equation

$$\begin{aligned} \mathbf{K}_N(\hat{\omega} - \omega) &= \mathbf{\Lambda}^{-1} \boldsymbol{\varepsilon} \\ \mathbf{K}_N &:= \begin{bmatrix} N^{1/2} & 0 & 0 \\ 0 & N^{1/2} & 0 \\ 0 & 0 & N^{3/2} \end{bmatrix} \\ \mathbf{\Lambda} &:= \begin{bmatrix} 1 & 0 & 0 \\ 0 & C & \frac{C}{2} \\ 0 & \frac{C}{2} & \frac{C}{3} \end{bmatrix} \\ \boldsymbol{\varepsilon} &:= \begin{bmatrix} \frac{1}{\sqrt{N}} \sum_{n=0}^{N-1} \operatorname{re} \{u(n)e^{-j4\eta(n)}\} \\ \frac{1}{\sqrt{N}} \sum_{n=0}^{N-1} \operatorname{im} \{u(n)e^{-j4\eta(n)}\} \\ \frac{1}{\sqrt{N}} \sum_{n=0}^{N-1} \left(\frac{n}{N}\right) \operatorname{im} \{u(n)e^{-j4\eta(n)}\} \end{bmatrix}. \end{aligned} \quad (39)$$

²The notations re and im stand for the real and imaginary part of a complex-valued number, respectively.

Since in (39) only $\boldsymbol{\varepsilon}$ is random, the asymptotic covariance matrix of $\hat{\omega}$ is given by

$$\begin{aligned} \boldsymbol{\Sigma}_{\hat{\omega}} &:= \lim_{N \rightarrow \infty} E \{ \mathbf{K}_N(\hat{\omega} - \omega)(\hat{\omega} - \omega)^T \mathbf{K}_N^T \} \\ &= \lim_{N \rightarrow \infty} E \{ \mathbf{\Lambda}^{-1} \boldsymbol{\varepsilon} \boldsymbol{\varepsilon}^T \mathbf{\Lambda}^{-1} \} = \mathbf{\Lambda}^{-1} \mathbf{R}_{\boldsymbol{\varepsilon}} \mathbf{\Lambda}^{-1} \end{aligned}$$

where $\mathbf{R}_{\boldsymbol{\varepsilon}} := \lim_{N \rightarrow \infty} E \{ \boldsymbol{\varepsilon} \boldsymbol{\varepsilon}^T \}$. Observe that

$$\begin{aligned} \mathbf{R}_{\boldsymbol{\varepsilon}}(1, 1) &= \lim_{N \rightarrow \infty} \frac{1}{N} E \left[\left(\sum_{n=0}^{N-1} \operatorname{re} \{u(n)e^{-j4\eta(n)}\} \right)^2 \right] \\ &= \lim_{N \rightarrow \infty} \frac{1}{4N} \sum_{n_1, n_2=0}^{N-1} E \left\{ \left[u(n_1)e^{-j4\eta(n_1)} + u^*(n_1)e^{j4\eta(n_1)} \right] \right. \\ &\quad \left. \cdot \left[u(n_2)e^{-j4\eta(n_2)} + u^*(n_2)e^{j4\eta(n_2)} \right] \right\}. \end{aligned}$$

Using (35) and (36), $\mathbf{R}_{\boldsymbol{\varepsilon}}(1, 1)$ can be written as

$$\mathbf{R}_{\boldsymbol{\varepsilon}}(1, 1) = \lim_{N \rightarrow \infty} \frac{1}{2N} \sum_{n=0}^{N-1} (D + B - 2C^2) = \frac{1}{2}(D + B - 2C^2).$$

Similarly, we obtain $\mathbf{R}_{\boldsymbol{\varepsilon}}(1, k) = 0$, $k = 2, 3$, which means that the NLS estimators of the amplitude and phase parameters are asymptotically decoupled.

To evaluate the asymptotic variance of $\hat{\omega}_l$, $l = 0, 1$, we need to compute for $k, m = 0, 1$, as shown in the equation at the bottom of the page. Using a technique similar to the one developed in the evaluation of $\mathbf{R}_{\boldsymbol{\varepsilon}}(1, 1)$, we obtain

$$\mathbf{R}_{\boldsymbol{\varepsilon}}(2+k, 2+m) = \frac{1}{2(k+m+1)}(B - D), \quad k, m = 0, 1.$$

$$\begin{aligned} &\sum_{n=0}^{N-1} \operatorname{re} \{u(n)e^{-j4\eta(n)}\} - N(\hat{C} - C) = 0 \\ &\sum_{n=0}^{N-1} n^k \operatorname{im} \{u(n)e^{-j4\eta(n)}\} - C \sum_{l=0}^1 (\hat{\omega}_l - \omega_l) \sum_{n=0}^{N-1} n^{k+l} = 0, \quad \text{for } k = 0, 1. \end{aligned}$$

$$\frac{1}{\sqrt{N}} \sum_{n=0}^{N-1} \operatorname{re} \{u(n)e^{-j4\eta(n)}\} = \sqrt{N}(\hat{C} - C) \quad (37)$$

$$\begin{aligned} \frac{1}{\sqrt{N}} \sum_{n=0}^{N-1} \left(\frac{n}{N}\right)^k \operatorname{im} \{u(n)e^{-j4\eta(n)}\} &= C \sum_{l=0}^1 N^{l+1/2} (\hat{\omega}_l - \omega_l) \left(\frac{1}{N} \sum_{n=0}^{N-1} \left(\frac{n}{N}\right)^{k+l} \right) \\ &= \sum_{l=0}^1 \frac{C}{k+l+1} N^{l+1/2} (\hat{\omega}_l - \omega_l), \quad k = 0, 1 \end{aligned} \quad (38)$$

$$\begin{aligned} \mathbf{R}_{\boldsymbol{\varepsilon}}(2+k, 2+m) &= \lim_{N \rightarrow \infty} \frac{1}{N} \sum_{n_1, n_2=0}^{N-1} \left(\frac{n_1}{N}\right)^k \left(\frac{n_2}{N}\right)^m \\ &\quad \cdot E \left[\operatorname{im} \{u(n_1)e^{-j4\eta(n_1)}\} \operatorname{im} \{u(n_2)e^{-j4\eta(n_2)}\} \right]. \end{aligned}$$

$$\begin{aligned}
E\{y_k(n)\} &= \int_0^\infty \int_{-\pi}^\pi \rho^k(n) e^{j4\phi(n)} f(\rho(n), \phi(n)) d\phi(n) d\rho(n) \\
&= \frac{1}{M\pi\sigma_v^2} \sum_{(l,p) \in \mathcal{A}_M} \sum_{m=0}^3 \int_0^\infty \rho^{k+1}(n) e^{-(1/\sigma_v^2)[\rho^2(n) + \varrho_{l,p}^2]} \\
&\quad \cdot \int_{-\pi}^\pi e^{j4\phi(n)} e^{(2\rho(n)\varrho_{l,p}/\sigma_v^2) \cos[\phi(n) - \psi_{l,p} - (m\pi/2) - \eta(n)]} d\phi(n) d\rho(n) \\
&= \frac{8}{M\sigma_v^2} e^{j4\eta(n)} \sum_{(l,p) \in \mathcal{A}_M} e^{j4\psi_{l,p}} \int_0^\infty \rho^{k+1}(n) e^{-(1/\sigma_v^2)[\rho^2(n) + \varrho_{l,p}^2]} I_4\left(\frac{2\rho(n)\varrho_{l,p}}{\sigma_v^2}\right) d\rho(n)
\end{aligned} \tag{42}$$

Thus, the matrix $\mathbf{R}_\mathcal{E}$ can be expressed as

$$\mathbf{R}_\mathcal{E} = \frac{1}{2} \begin{bmatrix} \mathcal{B} + \mathcal{D} - 2\mathcal{C}^2 & 0 \\ 0 & (\mathcal{B} - \mathcal{D})\mathbf{H} \end{bmatrix}$$

where $\mathbf{H} := \{1/(k+l+1)\}_{k,l=0}^1$ is the so-called Hilbert matrix [14]. Note that

$$\mathbf{\Lambda}^{-1} = \begin{bmatrix} 1 & 0 \\ 0 & \mathcal{C}^{-1}\mathbf{H}^{-1} \end{bmatrix}.$$

Therefore, the asymptotic covariance matrix of $\hat{\omega}$ is obtained as

$$\begin{aligned}
\Sigma_{\hat{\omega}} &= \mathbf{\Lambda}^{-1} \mathbf{R}_\mathcal{E} \mathbf{\Lambda}^{-1} \\
&= \frac{1}{2} \begin{bmatrix} \mathcal{B} + \mathcal{D} - 2\mathcal{C}^2 & 0 \\ 0 & (\mathcal{B} - \mathcal{D})\mathcal{C}^{-2}\mathbf{H}^{-1} \end{bmatrix}
\end{aligned} \tag{40}$$

where the inverse of the Hilbert matrix \mathbf{H} is given by [14]

$$\mathbf{H}^{-1}(k, l) = (-1)^{k+l} \frac{(k+2)!(l+2)!}{(k!)^2(l!)^2(1-k)!(1-l)!(k+l+1)}. \tag{41}$$

Based on (40) and (41), some direct computations lead to the sought asymptotic variances (15). This concludes the proof of Theorem 1.

APPENDIX III

DERIVATION OF EXPRESSIONS (31) AND (32)

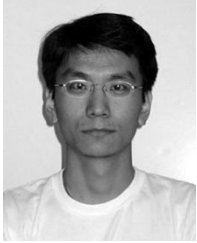
Using (5), we can obtain (42), at the top of the page, where in deriving the third equality in (42), we made use of the definition of $I_4(\cdot)$ [1, eq. (9.6.19)]. Note that the first term of the sum in (42) (i.e., $l = p = 0$ and $\psi_{0,0} = \pi/4$) can be written as

$$\begin{aligned}
&\frac{8}{M\sigma_v^2} e^{j4\eta(n)} e^{j4\psi_{0,0}} \\
&\cdot \int_0^\infty \rho^{k+1}(n) e^{-(1/\sigma_v^2)[\rho^2(n) + \varrho_{0,0}^2]} I_4\left(\frac{2\rho(n)\varrho_{0,0}}{\sigma_v^2}\right) d\rho(n) \\
&= -\frac{4\sigma_v^k}{M} \frac{1}{(\sqrt{2})^k} e^{j4\eta(n)} e^{-(\gamma/2)} \int_0^\infty \zeta^{k+1} e^{-(\zeta^2/2)} I_4(\alpha\zeta) d\zeta \\
&= -\frac{4\sigma_v^{k-4}}{M} e^{-(\varrho_{0,0}^2/\sigma_v^2)} \varrho_{0,0}^4 \frac{\Gamma(\frac{k}{2} + 3)}{\Gamma(5)} \Phi\left(\frac{k}{2} + 3, 5, \frac{\varrho_{0,0}^2}{\sigma_v^2}\right) e^{j4\eta(n)}
\end{aligned} \tag{43}$$

where $\alpha := \sqrt{2}\varrho_{0,0}/\sigma_v$, $\gamma := \alpha^2$, $\zeta := \sqrt{2}\rho(n)/\sigma_v$, $\Phi(\cdot, \cdot, \cdot)$ denotes the confluent hypergeometric function, and the last equality in (43) employs [10, eq. (6.643,2)] and [1, eq. (13.1.32)]. By exploiting the same procedure as in (43) on the other terms of $E\{y_k(n)\}$ in (42), we can obtain (31). The expression (32) for \mathcal{D}_k can be derived in a similar way.

REFERENCES

- [1] *Handbook of Mathematical Functions*, M. Abramowitz and I. A. Stegun, Eds., NBS, 1964.
- [2] O. Besson, M. Ghogho, and A. Swami, "Parameter estimation for random amplitude chirp signals," *IEEE Trans. Signal Processing*, vol. 47, pp. 3208–3219, Dec. 1999.
- [3] K. V. Cartwright, "Blind phase recovery in general QAM communication systems using alternative higher order statistics," *IEEE Signal Processing Lett.*, vol. 6, pp. 327–329, Dec. 1999.
- [4] —, "Blind phase recovery in cross QAM communication systems with eighth-order statistics," *IEEE Signal Processing Lett.*, vol. 8, pp. 304–306, Dec. 2001.
- [5] L. Chen, H. Kusaka, and M. Kominami, "Blind phase recovery in QAM communication systems using higher order statistics," *IEEE Signal Processing Lett.*, vol. 3, pp. 147–149, May 1996.
- [6] D. Efstathiou and A. H. Aghvami, "A comparison study of the estimation period of carrier phase and amplitude gain error for 16-QAM rayleigh faded burst transmission," in *GLOBECOM'94*, San Francisco, CA, 1994, pp. 1904–1908.
- [7] —, "Feedforward synchronization techniques for 16-QAM TDMA demodulations," in *Conf. Rec. ICC'96*, 1996, pp. 1432–1436.
- [8] C. N. Georghiades, "Blind carrier phase acquisition for QAM constellations," *IEEE Trans. Commun.*, vol. 45, pp. 1477–1486, Nov. 1997.
- [9] M. Ghogho and A. Swami, "Non-efficiency of the nonlinear least-squares estimator of polynomial phase signals in colored noise," in *Conf. Rec. Asilomar'98*, 1998, pp. 1447–1451.
- [10] I. S. Gradshteyn and I. M. Ryzhik, *Table of Integrals, Series, and Products*. New York: Academic, 1965.
- [11] T. Hasan, "Nonlinear time series regression for a class of amplitude modulated cosinusoids," *J. Time Series Analysis*, vol. 3, no. 2, pp. 109–122, 1982.
- [12] U. Mengali and A. N. D' Andrea, *Synchronization Techniques for Digital Receivers*. New York: Plenum, 1997.
- [13] M. Morelli, A. N. D' Andrea, and U. Mengali, "Feedforward estimation techniques for carrier recovery in 16-QAM modulation," in *Broadband Wireless Communications*, M. Luise and S. Pupolin, Eds. New York: Springer-Verlag, 1998.
- [14] K. S. Miller, *Some Eclectic Matrix Theory*. Melbourne, FL: Krieger, 1987.
- [15] M. Moeneclaey and G. de Jonghe, "MI-oriented NDA carrier synchronization for general rotationally symmetric signal constellations," *IEEE Trans. Commun.*, vol. 42, pp. 2531–2533, Aug. 1994.
- [16] B. E. Paden, "A matched nonlinearity for phase estimation of a PSK-modulated carrier," *IEEE Trans. Inform. Theory*, vol. IT-32, pp. 419–422, May 1986.
- [17] B. Picinbono and P. Bondon, "Second-order statistics of complex signals," *IEEE Trans. Signal Processing*, vol. 45, pp. 411–420, Feb. 1997.
- [18] F. Rice, B. Cowley, B. Moran, and M. Rice, "Cramér–Rao lower bound for QAM phase and frequency estimation," *IEEE Trans. Commun.*, vol. 49, pp. 1582–1591, Sept. 2001.
- [19] H. Sari and S. Moridi, "New phase and frequency detectors for carrier recovery in PSK and QAM systems," *IEEE Trans. Commun.*, vol. 36, pp. 1035–1043, Sept. 1988.
- [20] E. Serpedin, P. Ciblat, G. B. Giannakis, and P. Loubaton, "Performance analysis of blind carrier phase estimators for general QAM constellations," *IEEE Trans. Signal Processing*, vol. 49, pp. 1816–23, Aug. 2001.
- [21] P. Stoica and R. Moses, *Introduction to Spectral Analysis*. Englewood Cliffs, NJ: Prentice-Hall, 1997.
- [22] A. J. Viterbi and A. M. Viterbi, "Nonlinear estimation of PSK-modulated carrier phase with application to burst digital transmissions," *IEEE Trans. Inform. Theory*, vol. IT-29, pp. 543–551, July 1983.



Yan Wang received the B.S. degree in electronics from Peking University, China, in 1996, the M.Sc. degree in telecommunications engineering from Beijing University of Posts and Telecommunications (BUPT), China, in 1999, and is currently working toward the Ph.D. degree at Texas A&M University, College Station.

From 1999 to 2000, he was a Member of the BUPT-Nortel R&D Center, Beijing, China. Since 2000, he has been a Research Assistant with the Department of Electrical Engineering, Texas A&M University. His research interests are in the area of statistical signal processing and its applications in wireless communication systems.



Erchin Serpedin (S'96–M'99) received the Diploma of Electrical Engineering (with highest distinction) from the Polytechnic Institute of Bucharest, Bucharest, Romania, in 1991, the Specialization degree in signal processing and transmission of information from the Ecole Supérieure D'Electricité, Paris, France, in 1992, the M.Sc. degree from the Georgia Institute of Technology, Atlanta, in 1992, and the Ph.D. degree in electrical engineering from the University of Virginia, Charlottesville, in 1999.

From 1993 to 1995, he was an Instructor with the Polytechnic Institute of Bucharest, and from January to June 1999, he was a Lecturer at the University of Virginia. In July 1999, he joined the Department of Electrical Engineering, Texas A&M University, College Station, as an Assistant Professor. His research interests lie in the areas of statistical signal processing and wireless communications.

Dr. Serpedin received the National Science Foundation Career Award in 2001, and is currently an Associate Editor for the IEEE COMMUNICATIONS LETTERS and the IEEE SIGNAL PROCESSING LETTERS.



Philippe Ciblat was born in Paris, France, in 1973. He received the Engineer degree from the Ecole Nationale Supérieure des Télécommunications, Paris, France, 1996, the M.Sc. degree in signal processing from the University of Paris-Sud, Orsay, France, in 1996, and the Ph.D. degree from the University of Marne-la-Vallée, France, in 2000.

From October 2000 to June 2001, he was a Post-Doctoral Researcher with the Communications and Remote Sensing Department, Université Catholique de Louvain, Belgium. He is currently an Associate Professor in the Department of Communications and Electronics, Ecole Nationale Supérieure des Télécommunications, Paris, France. His research interests include statistical and digital signal processing, especially blind equalization and synchronization.